Contract No.:

This manuscript has been authored by Battelle Savannah River Alliance (BSRA), LLC under Contract No. 89303321CEM000080 with the U.S. Department of Energy (DOE) Office of Environmental Management (EM).

ARTICLE

Probing the hydrolytic degradation of UF_4 in humid air

Bryan J. Foley, [a] Jonathan H. Christian,[a]* Christopher A. Klug,[b‡] Eliel Villa-Aleman, [a] Matthew Wellons,[a] Michael DeVore II, [a] Nicholas Groden, [a] Jason Darvin[a]

Received 00th January 20xx,
Accepted 00th January 20xx

DOI: 10.1039/x0xx00000x

This manuscript describes the chemical transformations that occur during hydrolysis of uranium tetrafluoride (UF_4) due to its storage in humid air (85% and 50% relative humidity) at ambient temperatures. This hydrolysis was previously reported to proceed slowly or not at all (depending on the percent relative humidity); however, previous reports relied primarily on X-ray diffraction methods to probe uranium speciation. In our report, we employ a battery of physiochemical probing techniques to explore potential hydrolysis, including Raman spectroscopy, powder X-ray diffraction, ^{19}F nuclear magnetic resonance, scanning electron microscopy, and focused ion beam microscopy with energy-dispersive X-ray spectroscopy. Of these, only Raman spectroscopy proved to be particularly useful at observing chemical changes to UF_4. It was found that anhydrous UF_4 slightly oxidizes over the course of thirteen days to Schoepite-like uranium complexes and possibly UO_3. In contrast, UF_4 exposed to 50% relative humidity slightly decomposes into UO_2F_2, Schoepite-like uranium complexes, and possibly a high order uranium oxide that eluded chemical assignment (U_xO_y). Despite the rich chemical speciation observed in our Raman spectroscopy measurements, X-ray diffraction and ^{19}F NMR measurements on the same material showed no changes. Microscopy measurements suggest that the observed reactions between UF_4 and water occur primarily on the surface of UF_4 particulates via a method that is visually similar to surface corrosion of metals. Therefore, we postulate that NMR spectroscopy and X-ray diffraction, which are well-suited for bulk analysis, are less suited than Raman spectroscopy to observe the surface-based reactions that occur to UF_4 when exposed to humid air. Considering the importance of UF_4 in the production of nuclear fuel and weapons, the results presented herein are widely applicable to numerous nuclear science fields where uranium detection and speciation in humid environments is of value, including nuclear nonproliferation and nuclear forensics.

Introduction

Advancing the understanding of nuclear material synthesis and degradation pathways is vital to furthering nuclear non-proliferation efforts, environmental remediation, and nuclear forensics analysis.[1,2] Specific interests have been placed on understanding the behaviour of UF_4 when exposed to environmental elements (e.g., ultraviolet radiation, heat, and water).[3] Of these environmental factors, water is by far the most ubiquitous. As such, water-induced UF_4 degradation is of particular interest to the nuclear community, and recently, our group published two articles on the hydrolysis of anhydrous UF_4. In these articles, anhydrous UF_4 was submerged in water and the resulting formation of $UF_4(H_2O)_{2.5}$ was observed using a variety of characterization techniques.[4,5] Since UF_4 is a common chemical form used in the production of oxides for nuclear fuel, impurities in the UF_4 material, such as UO_2F_2, UO_3, U_3O_8, etc. are highly relevant to the production of high-quality UO_2 for use as nuclear fuel. Therefore, reaction of UF_4 with water has important implications in the area of applied nuclear science.

In most storage scenarios, UF_4 will be kept indoors away from rain, sun, and excessive heat/cold. This leaves ambient moisture (i.e., relative humidity) as the most likely environmental factor encountered by UF_4.[3b] Humidity induced degradation of various U-bearing nuclear fuel-related compounds have been studied previously.[6] However, to the best of our knowledge, there are only four published reports that have analyzed the degradation of UF_4 due to ambient moisture.[7] Of these four manuscripts, only one focused on chemical transformations of UF_4 in air with less than 100% relative humidity (RH) and no outside chemical interference.[7a] That report, by Pastoor et al., utilized thermogravimetric analysis and X-ray diffraction measurements to show that UF_4 remains stable in air at ≤ 75% RH for up to 9 months. However, under high humidity conditions (>90% RH), UF_4 was reported to form UF_4 hydrates within 30 days of humidity exposure. This contrasts with a report by Pointurier et al. that used micro-Raman spectroscopy to study the hydrolysis of UF_4 microparticles exposed to 100% RH in both air and argon.[7b] Pointurier and co-workers documented that UF_4 particles are stable to air, heat, and UV irradiation in the absence of moisture. However, UF_4 exposed to 100% RH was reported to undergo rapid transformation to uranyl hydroxide (Schoepite) and an undetermined compound. Importantly, no UF_4 hydrates

[a] Savannah River National Laboratory, Aiken, SC 29803
[b] Naval Research Laboratory, Washington, D.C. 20375
* Jonathan.Christian@srnl.doe.gov
‡ Christopher.klug@nrl.navy.mil
§Electronic Supplementary Information (ESI) available: [details of any supplementary information available should be included here]. See DOI: 10.1039/x0xx00000x

were observed after 3 months of exposure to air and argon at 100% RH.

Considering the differences in chemical transformations observed by micro-Raman spectroscopic analysis compared to X-ray diffraction on the same material, we were motivated to further explore the possibility of humidity-induced degradation of UF_4 on a bulk scale, at <100% RH, and using Raman spectroscopy and microscopy as our primary interrogation tools.

We found that UF_4 does degrade under both 85% and 50% RH conditions in air. While it is difficult to definitively assign chemical species to the Raman bands of the degradation products due to multiple uranium-bearing complexes exhibiting Raman bands at similar energies, we tentatively ascribe degradation products to UO_2F_2, UO_3, U_xO_y, and "Schoepite-like" uranium complexes. Degradation products were found to be different depending on the relative humidity environment (85% RH vs 50% RH). These results, when combined with previous studies[7] of humidity-induced degradation of UF_4, suggest that UF_4 hydrolysis involves a complex interplay between chemical, kinetic, and thermodynamic factors, which are perhaps best studied by vibrational spectroscopy, and which still warrant further investigation.

Results and Discussion

Commercially purchased anhydrous UF_4 was first characterized for its baseline properties by Raman spectroscopy (Figure S1), powder X-ray diffraction (pXRD; Figure S2), and scanning electron microscopy (SEM; Figure S3). Characterization data were consistent with previous reports on anhydrous UF_4.[4,8] Following baseline characterization, anhydrous UF_4 was segregated into five separate samples with ~10 mg of powder per sample. The first sample was placed in an incubation system which exposed the sample to ambient-temperature air at 85% relative humidity (RH) while daily in-situ Raman measurements were acquired. The second sample was placed in a similar incubation system and was exposed to ambient-temperature air at 50% RH while daily in-situ Raman measurements were conducted. The third sample was placed in a humidity chamber at ambient temperature and 85% RH while daily in-situ pXRD measurements were acquired. The fourth sample was placed in a humidity chamber at ambient temperature and 50% RH while daily in-situ pXRD measurements were conducted. The fifth sample was placed in a lab-made nuclear magnetic resonance (NMR) probe that permitted in-situ ^{19}F NMR measurements while exposing the sample to a saturated solution of KCl at 20 °C which results in a relative humidity environment of 85% with only a small variation of less than 1% per 5 °C.[9]

The Raman spectrum of anhydrous UF_4 prior to humidity exposure showed multiple bands between 100 – 400 cm^{-1} (Figure 1). Raman spectra acquired after one week at 85% RH showed the characteristic UF_4 spectrum plus slight in-growth of a broad band near 840 cm^{-1}; the intensity of this band increased with time. The broadness of this band may indicate the presence of different uranyl hydroxide and uranium oxide species. Uranium complexes that exhibit Raman bands in this range are collectively referred to as "Schoepite-like" and can be described by many different formulae. For example, $UO_2(OH)_2•H_2O$,[10] $UO_3•2(H_2O)$,[11] $UO_3•(2+x)H_2O$ ($x < 1$),[12] or $(UO_2)_4O(OH)_6•(H_2O)_6$.[13] Observation of the 840 cm^{-1} broad band is consistent with previously reported data from the hydrolysis of UO_2F_2, where a broad band centered at 846 cm^{-1} was resolved into three different uranium complexes (uranyl fluoride hydrate, uranyl hydroxide, and uranyl peroxide) after several months of water exposure.[3b] Because our experiment did not proceed for months, such resolution of the broad band at 840 cm^{-1} observed in our Raman spectra, whether achievable or not, was precluded.

Starting around day five, the characteristic UF_4 bands centered at ~130 cm^{-1} and ~170 cm^{-1} increased in intensity (denoted by the asterisks in Figure 1) Additionally, a shoulder peak appeared to grow in near 150 cm^{-1} and a broad band emerged at 750 cm^{-1}. This spectral evolution is shown in Figure 1 (Top). It is unclear what led to the relative intensity increase of the 130 cm-1 and 170 cm-1bands; however, we believe the growth me be attributable to ingrowth of uranyl fluoride hydrate.[14] As shown in Table S1, UO_2F_2 hydrate has a vibrational mode at 174 cm^{-1}, which is quite close to 170 cm^{-1}. However, UO_2F_2 hydrate also exhibits an intense Raman band at 867 cm^{-1} which was not observed in these spectra, although the 867 cm^{-1} region is largely obscured by the broad band centered near 840 cm^{-1}.

The broad band centered near ~750 cm^{-1} became very evident after 11 days of exposure to 85% RH. As shown in Table S1, a band near 750 - 768 cm^{-1} has been previously observed in Raman spectra of both U_3O_8 and UO_3. To assign the chemical origin of our 750 cm^{-1} band, it is necessary to look for the presence or absence of other characteristic Raman bands for suspected compounds and to consider the relative intensities of those bands. While Butler et al. show that U_3O_8 produces a Raman band at 752 cm^{-1}, they also show that U_3O_8 produces Raman bands at 236, 342, 408, 480, 638, 798, and 888 cm^{-1}.[15] None of these bands were observed in our Raman spectra, even though many of these bands are of greater relative intensity than the 752 cm^{-1} band. On the other hand, Palacios et al. found that γ-UO_3 produces Raman bands at 768 and 846 cm^{-1}.[16] The band at 768 cm^{-1} has a much higher relative intensity than the band at 846 cm^{-1} which is consistent with our observation of a broad band centered at 750 cm^{-1} and a shoulder embedded in the broad band near 840 cm^{-1}. Thus, we have tentatively assigned the feature near 750 cm^{-1} to UO_3. In total, the observation of Schoepite-like complexes, and possibly UO_3 in our Raman spectra, clearly indicates that humidity-based degradation occurs to UF_4 at room-temperature and 85% RH.

Conversely, pXRD measurements obtained on UF_4 exposed to 85% RH showed no change had occurred in the material (Figure S4). This observation is in stark contrast to our Raman results, yet quantitative Rietveld analysis on the obtained pXRD data confirmed the purity of the UF_4 phase. Our Rietveld analysis agrees with the recent report by Pastoor et al., in which, quantitative phase analysis of pXRD data found UF_4 to be stable over the course of months when stored at room-temperature and <90% RH.[7a]

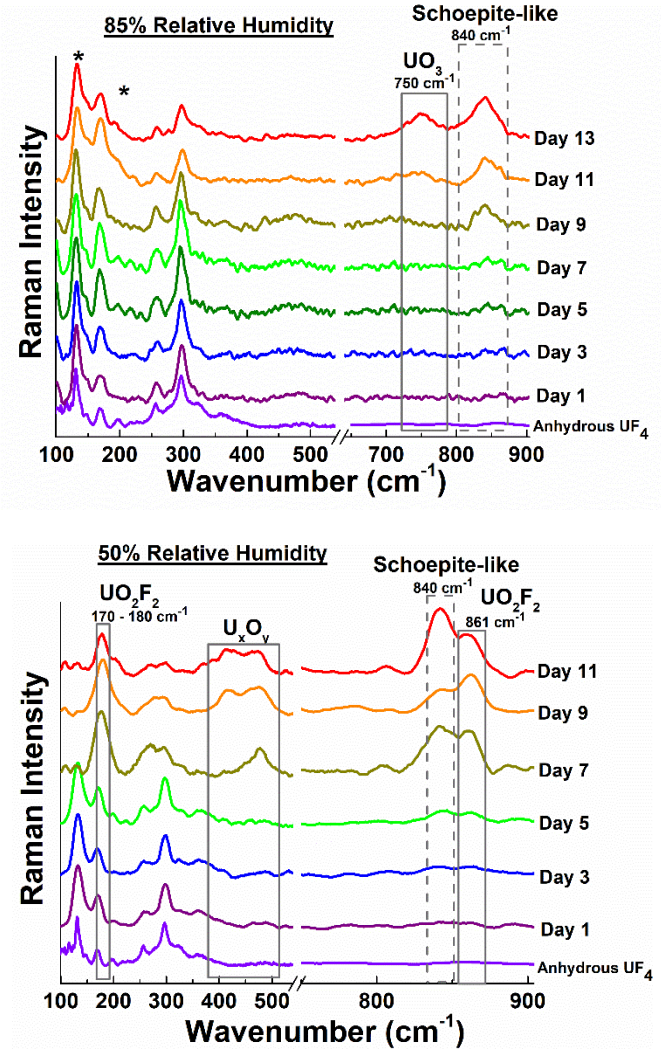

Figure 1. Top: Raman spectra of UF_4 at 85% RH as measured for 13 days. Characteristic UO_2F_2, Schoepite region, and UO_3 bands are annotated. Bottom: Raman spectra of UF_4 at 50% RH as measured for 11 days. Characteristic UO_2F_2, Schoepite region, and U_xO_y bands are denoted.

Raman spectra obtained from exposing UF_4 to 50% RH were different from those obtained at 85% RH. As shown in Figure 1 (Bottom), Raman measurements obtained after 1 day of exposure to 50% RH showed minor in-growth of bands at 861 and between 170 - 180 cm^{-1}. As stated above, these bands likely correspond to UO_2F_2 hydrate.**Error! Bookmark not defined.** This Raman spectrum also contains the broad band at 840 cm^{-1} corresponding to Schoepite-like complexes of uranium; however, in this case, the band does not obscure the energy region around the UO_2F_2 band. Another interesting Raman spectral feature from the 50% RH experiments is the emergence of a broad band at 440 cm^{-1} which has been tentatively assigned to higher order U_xO_y compounds based on comparison with previously published spectra.[15-17]

Despite the rich chemical speciation observed by Raman spectroscopy, pXRD measurements exhibited no changes when UF_4 was exposed to 50% RH (Figure S5). The diffraction data for UF_4 exposed to 50% RH was similar to diffraction data for anhydrous UF_4 as confirmed by Rietveld analysis. This is similar to our 85% RH pXRD measurements and is consistent with the recent report by Pastoor et al.[7a]

Attempts at using ^{19}F nuclear magnetic resonance (NMR) to observe chemical changes in UF_4 were not fruitful. Although the presence of paramagnetic U^{4+} causes the ^{19}F spin-lattice relaxation time to be very short, allowing for rapid spectral acquisition with good signal-to-noise, the ^{19}F resonances are fairly broad and no changes were observed in them after 14 days of humidity exposure (Figure S6). Observation of these broad spectroscopic features is consistent with literature precedent for UF_4 ^{19}F NMR spectroscopy.[18]

Considering that chemical changes to UF_4 were observed at 85% and 50% RH using Raman spectroscopy, but no changes were observed by us and Pastoor et al. using pXRD, we hypothesized that humidity-induced degradation likely occurs on the surface of UF_4 particles. Because of this, we suspect that both ^{19}F NMR spectroscopy and X-ray diffraction, which are well-suited for bulk analysis, are less optimal than Raman spectroscopy for studying the hydrolysis of UF_4.

To better understand the morphological changes that occur during UF_4 hydrolysis, SEM micrographs were acquired for UF_4 both before (Figure 3A) and after humidity exposure. After exposure to 85% RH (Figure 3B) and 50% RH (Figure 3C), the smooth, spherical feature of anhydrous UF_4 particles became irregular, rough, and etched.[19] Degradation largely began on the surface of the material and then penetrated somewhat into the spheroid.

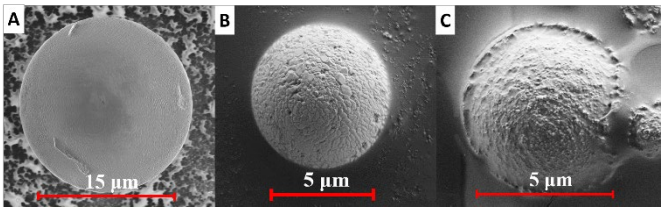

Figure 3. Scanning electron micrograph images of a) Representative sphere of anhydrous UF_4; b) Representative UF_4 sample after exposure to air at 85% RH for 13 days; c) Representative UF_4 sample after exposure to air at 50% RH for 11 days.

Focused ion beam (FIB) microscopy with energy-dispersive X-ray spectroscopy (EDS) was used to further evaluate the morphology and composition of a single particle of UF_4 exposed to 85% RH for thirteen days. These data show that oxygen may be present at the particle surface, although the amount relative to fluorine is extremely small, such that the EDS signal from oxygen is of a low signal-to-noise ratio (Figure 4 and Figure S8). Assignment of oxygen on the surface of the UF_4 particle from EDS alone would be dubious; however, in conjunction with our Raman results we believe these oxygen EDS signals to be genuine, albeit of low intensity. This further highlights the utility of Raman spectroscopy for identifying minor constituents in chemical mixtures, such as these oxygen-bearing moieties.

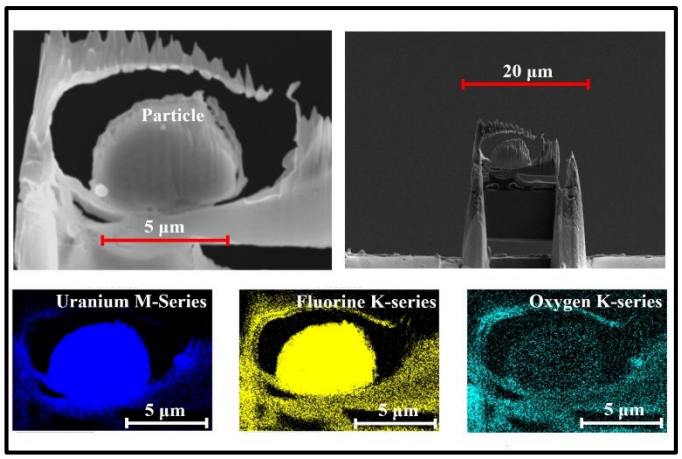

Figure 4. Energy-dispersive X-ray spectroscopy measurements of a single particle of UF_4 after 13 days in air at 85% RH. Images were taken on a single particle that was milled with a focused ion beam of gallium ions. Top: Mounted UF_4 particle Bottom: Composition determination by elemental color mapping; blue identifies uranium, yellow identifies fluorine, and teal identifies oxygen.

Conclusions

Commercially purchased uranium tetrafluoride was exposed to room-temperature air at 85% and 50% relative humidity. Raman spectroscopy revealed that UF_4 clearly degrades upon exposure to ambient moisture. Specific degradation products are tentatively assigned to multiple U-bearing oxides.

After exposure to 85% RH, the formation of Schoepite-like complexes and possibly UO_3 was observed. After exposure to 50% RH, UF_4 appears to form UO_2F_2 and Schoepite-like complexes in addition to a higher order uranium oxide (U_xO_y). Observation of the broad Schoepite-like band in Raman measurements of both 50% and 85% RH samples is uninformative in terms of identifying the specific chemical form of the degradation products; however, this would seem to indicate that UF_4 hydrolytically degrades to complex oxide/hydroxide complexes within two weeks of exposure to humid air.

The chemical changes observed in UF_4 throughout this manuscript are tentatively assigned by Raman spectroscopy. Measuring quality Raman spectra of UF_4 without degrading the sample requires low laser power and long integration times. Integration time is lengthened as the spectral window broadens. As hydrolytic degradation of UF_4 is a dynamic process, it is critical that the required integration time is relatively short such that the presented spectra show a snapshot of the status of the UF_4 material and not a blend of changes over many hours. To achieve this, the spectral window of the Raman spectra presented herein have been truncated. Using the Raman signatures in the 100-1000 cm^{-1} range, we have attempted to assign the degradation products to materials which logically follow the breakdown of UF_4 in humid air. However, assignment of some bands becomes complicated as multiple uranium-bearing complexes exhibit Raman bands at similar energies.

Both powder X-ray diffraction and nuclear magnetic resonance measurements were not useful for observing subtle hydrolytic changes incurred by UF_4 at both 50% and 85% RH. This is in excellent agreement with previously published results which found that UF_4 appears highly stable to ambient humidity when it is analyzed by pXRD.[7a]

Formation of oxide species at the surface of UF_4 following humidity exposure was confirmed using FIB microscopy and degradation/etching of the UF_4 surface was observed by SEM imaging.

The sum of all measurements presented herein leads to following conclusions:

1) Hydrolysis of UF_4 particles starts with surface degradation that is not easily measured by X-ray diffraction or ^{19}F NMR spectroscopy.
2) Raman spectroscopy is an excellent tool for measuring humidity-induced degradation of UF_4.
3) Degradation seems to produce several U-bearing oxides; however, definitive assignment is difficult due to overlapping or very similar Raman bands.

There is still room for exploration in the subject of UF_4 hydrolytic degradation in both experimental and computational space. Experimentally, options include infrared spectroscopy measurements, analysis of higher energy vibrational modes in the Raman spectra, and luminescence spectroscopy. Computationally, DFT investigation into the hydrolytic degradation of UF_4 without further experimental results may prove difficult. For example, when considering DFT calculations of one compound observed in this report, UO_3, one would need to calculate the vibrational modes of many polymorphs of this material and each of the corresponding hydrated structures. To this end, with additional efforts, there may be a potential synergy between future experimental results and DFT calculation efforts.

While the near indefinite stability of UF_4 as a solid has been previously reported,[20] herein we provide yet another disclosure of the water sensitivity of UF_4 in a controlled environment. As evidence of UF_4 hydrolytic sensitivity mounts, one must consider that UF_4 (of varying surface area) produced and stored in different locations around the world with different climates, ventilation systems, and humidities will behave differently. As such, exposure of UF_4 to ambient moisture in a chamber where humidity is continually applied may be considered a "stress-test" of sorts that has real-world applications.

Conflicts of interest

There are no conflicts to declare.

Acknowledgements

This work was supported by the Laboratory Directed Research and Development (LDRD) program and Discovery Science program within the Savannah River National Laboratory (SRNL). This work was produced by Battelle Savannah River Alliance, LLC under Contract No. 89303321CEM000080 with the U.S. Department of Energy. Publisher acknowledges the U.S. Government license to provide public access under the DOE

Public Access Plan (http://energy.gov/downloads/doe-public-access-plan).

Experimental Methods

General Considerations

Caution: *The UF_4 in these experiments contains natural uranium. Standard precautions for handling radioactive materials are recommended.*

Anhydrous UF_4 was purchased from International Bio-Analytical Industries, Inc. and was stored in a temperature and humidity-controlled chamber (<5% RH). This UF_4 was produced through an anhydrous hydrofluorination reaction with HF. Microscopy of this product showed the morphology of the UF_4 particles to be microspheres (Figure S3).

Nuclear Magnetic Resonance (NMR)

^{19}F NMR spectra and relaxation rates were obtained for UF_4 under static (i.e., non-spinning) conditions at room temperature and low field (2.35 T) using specially designed sample holders and probes which allowed *in situ* exposure to fixed humidity conditions (Figure S7). All experiments were performed using an Oxford superconducting magnet with a maximum field of 2.35 T and a 110 mm diameter room temperature bore. The specially designed NMR probe was attached to a Thorlabs linear translation stage (LNRS/M) which was mounted vertically underneath the magnet. LabVIEW software (National Instruments) in combination with a Thorlabs stepper motor controller (BSC201) was used to control the vertical motion of the NMR probe. The NMR spectrometer was based on a Tecmag Redstone console. High power RF pulses were obtained via an AR 1000LPM8. The preamp was Miteq AU-1313. ^{19}F NMR calibration using liquid hexafluorobenzene was achieved via a two-pulse Hahn echo experiment where the second pulse length was held fixed at 1.6 µs while the length of the first pulse was varied. Each data point was the sum of 128 scans with a wait time between scans of 8s. The ^{19}F NMR resonance frequency was 94.31 MHz. Optimal pulse lengths were determined from these data.

Custom glassware was fashioned which allowed the acquisition of *in situ* NMR spectra at a given humidity. The sample was sealed in the apparatus residing near a bulb of saturated KCl solution (Figure S7).[9] This solution, according to ASTM procedure E104-20,[21] can maintain 85% RH in a closed vessel with a variation of <1% per 5 °C. The sample glassware was inserted into a specially made NMR probe during measurements. For all NMR measurements, the sample was contained in a small tube surrounded by a 3-turn RF coil with a diameter of 5 mm (Figure S7). Pulse lengths of the custom probe were calibrated for optimal signal excitation and detection.

Raman Spectroscopy

Raman spectra were acquired on a LabRAM HR800 UV (Horiba Jobin-Yvon) equipped with an Andor 970N-UVB detector with a 1600 × 200 pixel array and 16 µm pixel resolution, and an InVia (Renishaw) Raman spectrometer equipped with a UV-enhanced deep depletion CCD detector. The excitation laser wavelength was λ = 785 nm (Note: When performing Raman spectroscopy measurements of UF_4, it is important that the laser excitation wavelength is away from the fluorescence absorption bands of UF_4. To date, 514 nm and 785 nm are among the more ideal laser excitation wavelengths to use when studying UF_4[8a]). The laser power ranged from 100 µW to 3 mW. The integration time varied from a few seconds to several hours for a high signal to noise ratio. For each integration time, at least two spectra were co-added to remove the contribution of cosmic rays to the spectra. For *in situ* Raman measurements, the RH values for each sample were maintained using an Okolab electric stage incubation system capable of maintaining a desired humidity level within ±1%.

Powder X-ray Diffraction (pXRD).

Powder X-ray diffraction (pXRD) measurements were acquired using a Rigaku Ultima IV powder X-ray diffractometer with a multi-sample changer attachment. X-rays were produced from a copper target at 40 kV and 44 mA. Scattered X-rays were detected using a D/teX Ultra semi-conductor detector with a Cu Kβ filter, with the tube/detector operated in the focusing beam (Bragg Brentano) method. On the incident side of the beam, the divergence slit was set at 2/3° and the divergence height limit slit at 10 mm while the scattering slit was set at 8.0 mm and the receiving slit was open on the diffracted side of the beam. The sample substrate was a 1-inch silicon disk cut along the (510) crystal plane to minimize background reflections. Paraffin wax is used to secure the powders to the substrate. The 2θ scan range was from 5 - 80° at a scan rate of 0.1° per minute. Measurements were performed with a stationary sample holder. XRD scans were analyzed with PDXL (Rigaku). A qualitative analysis of diffraction patterns was performed using search-match identification of the experimental XRD pattern to the ICDD database of crystal and powder X-ray diffraction pattern using the peak intensity and peak position.[22]

Scanning Electron Microscopy (SEM)

A Zeiss Supra 40 VP FEG-SEM utilizing SmartSEM software acquired the included micrographs under high-vacuum conditions. High resolution microscopy analyses consisted of secondary electron detection with the standard 30 µm aperture. Images were obtained at magnifications ranging from 600 – 21,000x with accelerating voltages ranging from 1.0 – 20.0 kV.

Focused Ion Beam Microscopy (FIB) and Energy-Dispersive X-ray Spectroscopy (EDS).

Micrographs of single milled UF_4 particles were obtained using an NB5000 Nanodue't double beam microscope with energy dispersive X-ray spectroscopy. Milling was conducted with 40 kV gallium ions with a 5 nm resolution at 40 kV.

ORCID Identifiers

Jonathan H. Christian: 0000-0003-1967-4841
Michael DeVore II: 0000-0002-1770-4472
Bryan J. Foley: 0000-0003-0570-769X
Matthew Wellons: 0000-0002-7172-2006
Eliel Villa-Aleman: 0000-0002-2891-0861

Notes and references

[1] Development and implementation support programme for nuclear verification 2020–2021. International Atomic Energy Agency, 2020.

[2] M. J. Kristo, A. M. Gaffney, N. Marks, K. Knight, W. S. Cassata, and I. D. Hutcheon, Nuclear Forensic Science: Analysis of Nuclear Material Out of Regulatory Control, *Annu. Rev. Earth Planet. Sci.* 2016, **44**, 555-579.

[3] a) M. Said and A. E. Hixon, Microscopy and spectroscopy of plutonium dioxide aging under ambient and near-ambient conditions, *J. Alloys Compd.*, 2021, **854**, 156277. b) M. C. Kirkegaard, M. W. Ambrogio, A. Miskowiec, A. E. Shields, J. L. Niedziela, T. L. Spano, and B. B. Anderson, Characterizing the degradation of $[(UO_2F_2)(H_2O)]_7 4H_2O$ under humid conditions, *J. Nucl. Mater.* 2019, **529**, 151889. c) D. Féron, in *Nuclear Corrosion Science and Engineering*, Woodhead Publishing, 2012, 2, 31-56.

[4] J. H. Christian, C. A. Klug, M. DeVore II, E. Villa-Aleman, B. J. Foley, N. Groden, A. T. Baldwin, and M. S. Wellons, Characterizing the solid hydrolysis product, $UF_4(H_2O)_{2.5}$, generated from neat water reactions with UF_4 at room temperature, *Dalton Trans.*, 2021, **50**, 2462-2471.

[5] A. Miskowiec, K. J. Pastoor, J. H. Christian, J. L. Niedziela, B. J. Foley, S. Isbill, A. E. Shields, L. L. Daemen, E. Novak, E. Nykwest, T. Spano, M. S. Wellons, M. Jensen, and J. Shafer, Inelastic Neutron Spectra of Uranium Tetrafluoride Hydrate $UF_4(H_2O)_{2.5}$, *J. Phys. Chem. C*, 2021, **125**, 25007-25021.

[6] Humidity-based hydrolytic reactions of other U-containing nuclear fuel-related compounds have been studied. See: a) M. C. Kirkegaard, T. L. Spano, M. W. Ambrogio, J. L. Niedziela, A. Miskowiec, A. E. Shields, and B. B. Anderson, Formation of a uranyl hydroxide hydrate via hydration of $[UO_2F_2)(H_2O)]_7 \bullet 4H_2O$, *Dalton Trans.*, 2019, **48**, 13685. b) M. C. Kirkegaard, A. Miskowiec, M. W. Ambrogio, and B. B. Anderson, Evidence of a Nonphotochemical Mechanism for the Solid-State Formation of Uranyl Peroxide, *Inorg. Chem.* 2018, **57**, 5711-5715. c) A. L. Tamasi, K. S. Boland, K. Czerwinski, J. K. Ellis, S. A. Kozimor, R. L. Martin, A. L. Pugmire, D. Reilly, B. L. Scott, A. D. Sutton, G. L. Wagner, J. R. Walensky, and M. P. Wilkerson, Oxidation and Hydration of U_3O_8 Materials Following Controlled Exposure to Temperature and Humidity, *Anal. Chem*. 2015, **87**, 4210-4217.

[7] a) K. J. Pastoor, M. J. Dzara, S. Pylypenko, J. C. Shafer, and M. P. Jensen, Chemical transformations of UF_4 under controlled temperature and relative humidity, *J. Nucl. Mater.*, 2021, **557**, 153260. b) F. Pointurier, C. Lelong, and O. Marie, Study of the chemical changes of µm-sized particles of uranium tetrafluoride (UF_4) in environmental conditions by means of micro-Raman spectrometry, *Vib. Spectrosc.*, 2020, **110**, 103145. c) J.-R. Zhong, L. Shao, C.-R. Yu, and Y.-M. Ren, In-situ FT-IR Study of Hydrolyzation Reaction at Ambient Temperature and Thermal Transformation Behaviors of UF_4/KBr in Air, *Acta Phys.-Chim. Sin.*, 2015, **31**, 2251-2258. d) J.-R. Zhong, L. Shao, C.-R. Yu, and Y.-M. Ren, Study of Thermal Chemical Reaction of UF_4 in Air, O_2, and Hydrated O_2, *Acta Phys.-Chim Sin.* 2015, **31**, 25-31.

[8] a) E. Villa-Aleman and M. S. Wellons, Characterization of uranium tetrafluoride (UF_4) with Raman spectroscopy, *J. Raman Spectrosc.*, 2016, **47**, 865-870. b) S. Kern, J. Hayward, S. Roberts, J. W. R. Jr., F. J. Rotella, L. Soderholm, B. Cort, M. Tinkle, M. West, D. Hoisington and G. H. Lander, *J. Chem. Phys.*, 1994, **101**, 9333–9337. c) *PDF 4 Database*, International Centre for Diffraction Data, Newtown Square, PA, 2015, Card No #01-082-2317.

[9] L. Greenspan, Humidity fixed points of binary saturated aqueous solutions, *J. Res. Natl. Bur. Standards – A, Phys. Chem.* 1967, **81**, 89-96.

[10] M. E. Torrero, I. Casas, J. de Pablo, M. C. A. Sandino, and B. Grambow, A Comparison Between Unirradiated UO_2(s) and Schoepite Solubilities in 1 M NaCl Medium, *Radiochim. Acta*, 1994, **66/67**, 29-35.

[11] A. G. Sowder, S. B. Clark, and R. A. Fjeld, The Effect of Silica and Phosphate on the Transformation of Schoepite to Becquerelite and Other Uranyl Phases, *Radiochim. Acta*, 1996, **74**, 45-49.

[12] L. E. Sweet, T. A. Blake, C. H. Henager Jr., S. Hu., T. J. Johnson, D. E. Meier, S. M. Peper, and J. M. Schwantes, Investigation of the polymorphs and hydrolysis of uranium trioxide, *J. Radioanal, Nucl. Chem.*, 2013, **296**, 105-110.

[13] a) J. Plášil, The crystal structure of uranyl-oxide mineral schoepite, $[(UO_2)_4O(OH)_6](H_2O)_6$, revisited, *J. Geosciences*, 2018, **63**, 65-73. b) R. L. Frost, J. Čejka, and M. L. Weier, Raman spectroscopic study of the uranyl oxyhydroxide hydrates: becquerelite, billietite, curite, schoepite, and vandendriesscheite, *J. Raman Spectrosc.* 2007, **38**, 460-466.

[14] D. P. Armstrong, R. J. Jarabek, and W. H. Fletcher, Micro-Raman Spectroscopy of Selected Solid $U_xO_yF_z$ Compounds, *Appl. Spectrosc.*, 1989, **43**, 461-468.

[15] I. S. Butler, G. C. Allen, and N. A. Tuan, Micro-Raman spectrum of triuranium octoxide, U_3O_8, Appl. Spectrosc., 1988, **42**, 901-902.

[16] M. L. Palacios and S. H. Taylor, Characterization of Uranium Oxides Using *in situ* Micro-Raman Spectroscopy, *Appl. Spectrosc.* 2000, **54**, 1372-1378

[17] D. Ho Mer Lin, D. Manara, P. Lindqvist-Reis, T. Fanghänel, and K. Mayer, The use of different dispersive Raman spectrometers for the analysis of uranium compounds, *Vib. Spectros.* 2014, **73**, 102-110.

[18] a) S. P. Gabuda, L. G. Falaleeva, and Y. V. Gagarinskii, Dipolar Broadening of the NMR Spectrum of ^{19}F in UF_4, *Physica Status Solidi (b)*, 1969, **33**, 435-438. b) M. Pintar, NMR Evidence for Contact Hyperfine Coupling in Paramagnetic UF_4, *Physica Status Solidi (b)*, 1966, **14**, 291-295. c) C. A. Klug and J. B. Miller, Automated detection of broad NMR spectra: ^{19}F NMR of paramagnetic UF_4 and ^{195}Pt NMR of supported Pt catalysts, *Solid State Nucl. Magn. Reson.*, 2018, **92**, 14-18. d) S. P. Gabuda, A. A. Matsutsin, and G. M. Zadneprovskii, NMR and the Structure of Uranium Tetrafluoride Crystal Hydrates, *Zh. Strukt. Khim.* 1969, **10**, 996-998.

[19] L. A. Giannuzzi, M. DeVore II, M. Summer, and M. Wellons, Micromanipulation, FIB, STEM, EDS and EELS of UF_4 Particles, *Microsc. Microanal.*, 2019, **25**, 1584-1585.

[20] N. S. Nikolaev and Y. A. Luk'yanychev, The Hydrolysis of Uranium Tetrafluoride UF_4, *Atomnaya Energiya*, 1961, **11**, 67-69.

[21] ASTM International, Designation: E104-20, Standard Practice for Maintaining Constant Relative Humidity by Means of Aqueous Solutions, Approved March 1, 2020.

[22] S. Gates-Rector and T. Blanton, The Powder Diffraction File: a quality materials characterization database, *Powder Diffraction*, 2019, **34**, 352-360.

Electronic Supporting Information

Probing the hydrolytic degradation of UF_4 in humid air

Bryan J. Foley,[a] Jonathan H. Christian,[a] Christopher A. Klug,[b‡] Eliel Villa-Aleman,[a] Matthew Wellons,[a] Michael DeVore II,[a] Nicholas Groden,[a] Jason Darvin[a]*

[a] *Savannah River National Laboratory, Aiken, SC 29803*
[b] *Naval Research Laboratory, Washington, D.C. 20375*
* Jonathan.Christian@srnl.doe.gov
‡ Christopher.klug@nrl.navy.mil

List of SI Figures

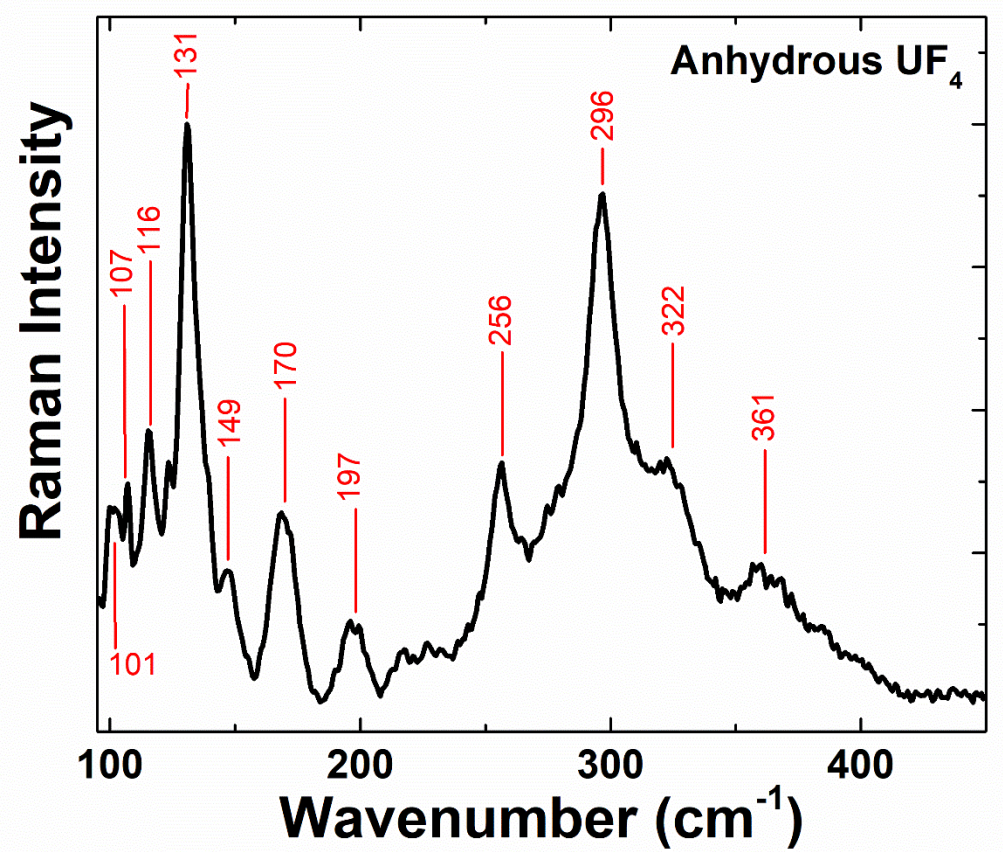

Figure S1. Raman spectrum of commercially-purchased UF_4 taken upon receipt.

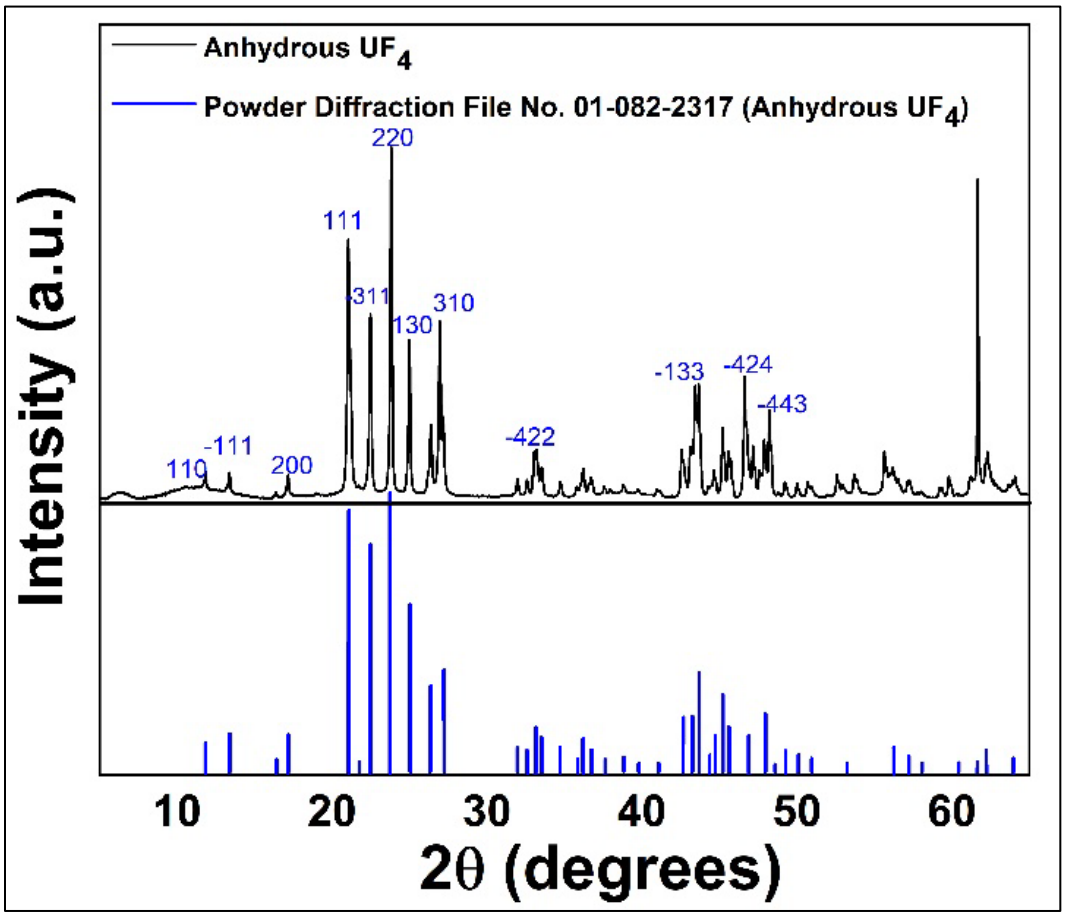

Figure S2. TOP: pXRD pattern of commercially purchased UF_4 obtained upon receipt (Note: The intense reflection at ~62° is an errant reflection from the sample holder). Miller Indices labels are shown above several of the more intense diffraction lines. Bottom: Database powder diffraction file for anhydrous UF4.[1]

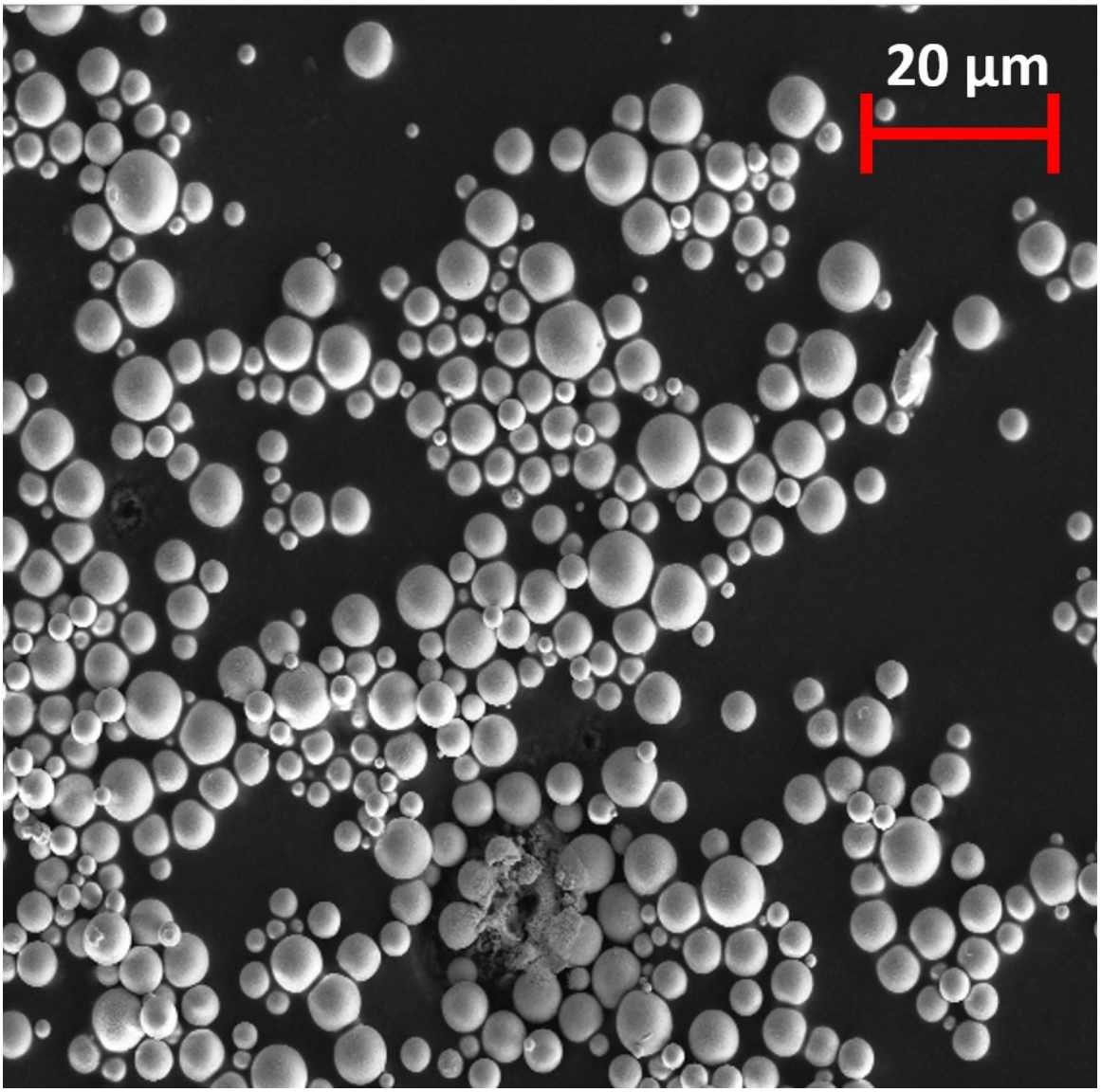

Figure S3. SEM image of commercially purchased UF_4 obtained upon receipt.

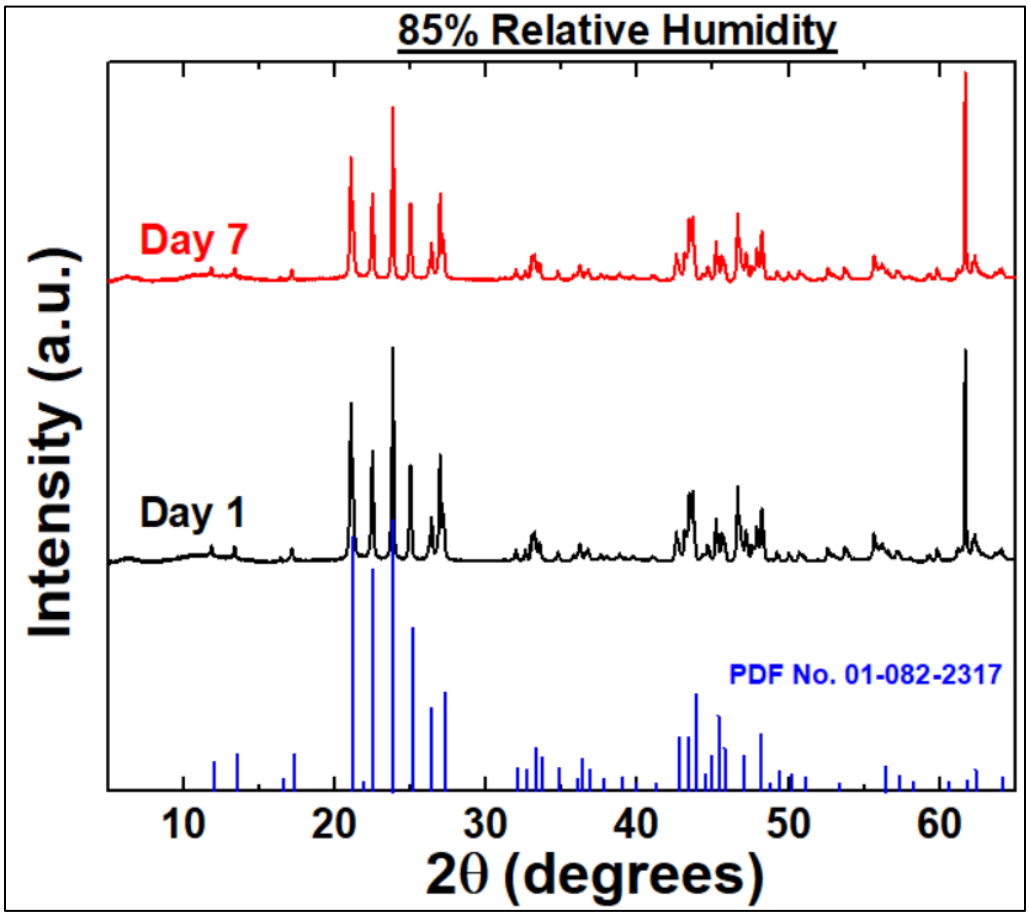

Figure S4. Bottom: Database powder diffraction file for anhydrous UF_4.[1] Middle: pXRD pattern of commercially purchased UF_4 after 1 day of exposure to 85% RH (Note: The intense reflections at 62° is an errant reflection from the sample holder). Top: pXRD pattern of commercially purchased UF_4 after 7 days of exposure to 85% RH (Note: The intense reflections at 62° is an errant reflection from the sample holder).

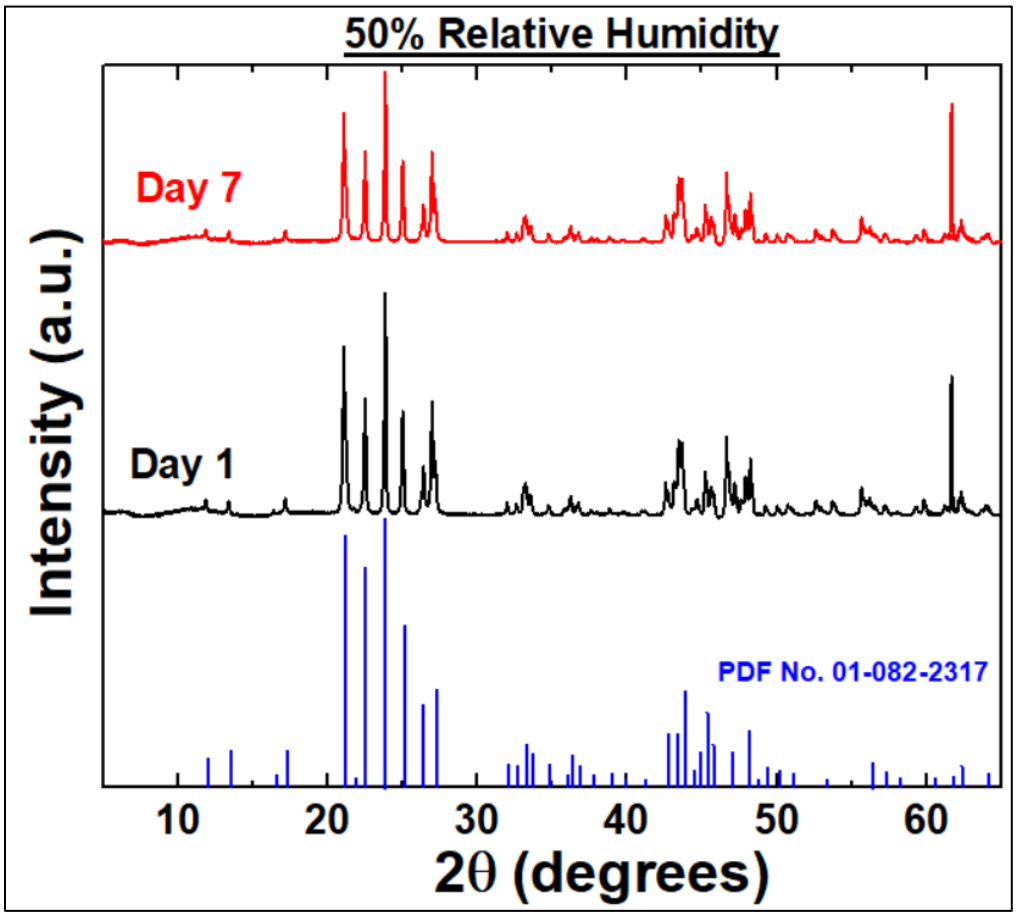

Figure S5. Bottom: Database powder diffraction file for anhydrous UF_4.[1] Middle: pXRD pattern of commercially purchased UF_4 after 1 day of exposure to 50% RH (Note: The intense reflections at 62° is an errant reflection from the sample holder). Top: pXRD pattern of commercially purchased UF_4 after 7 days of exposure to 50% RH (Note: The intense reflections at 62° is an errant reflection from the sample holder).

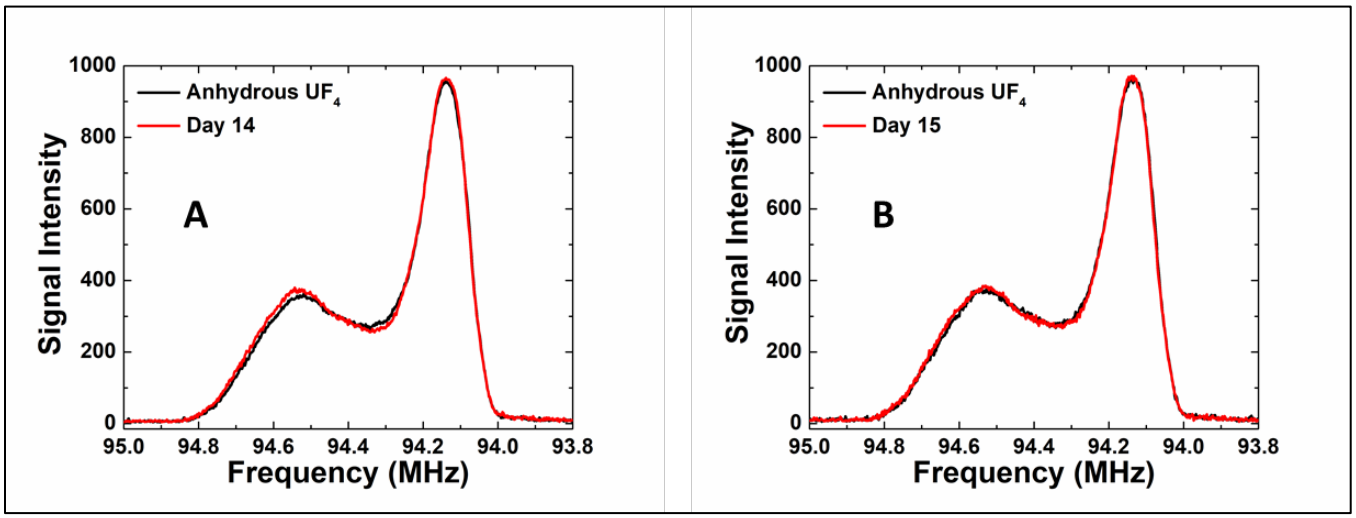

Figure S6. ^{19}F NMR spectra of UF_4 before (black trace) and after (red trace) exposure to air at 85% RH. These spectra resulted from the sum of 11 sub-spectra using an automated acquisition method a) with a wait time of 4 ms between scans; b) with a wait time of 4 s between scans. The total number of scans for each sub-spectrum was a) 2048 and b) 1024.

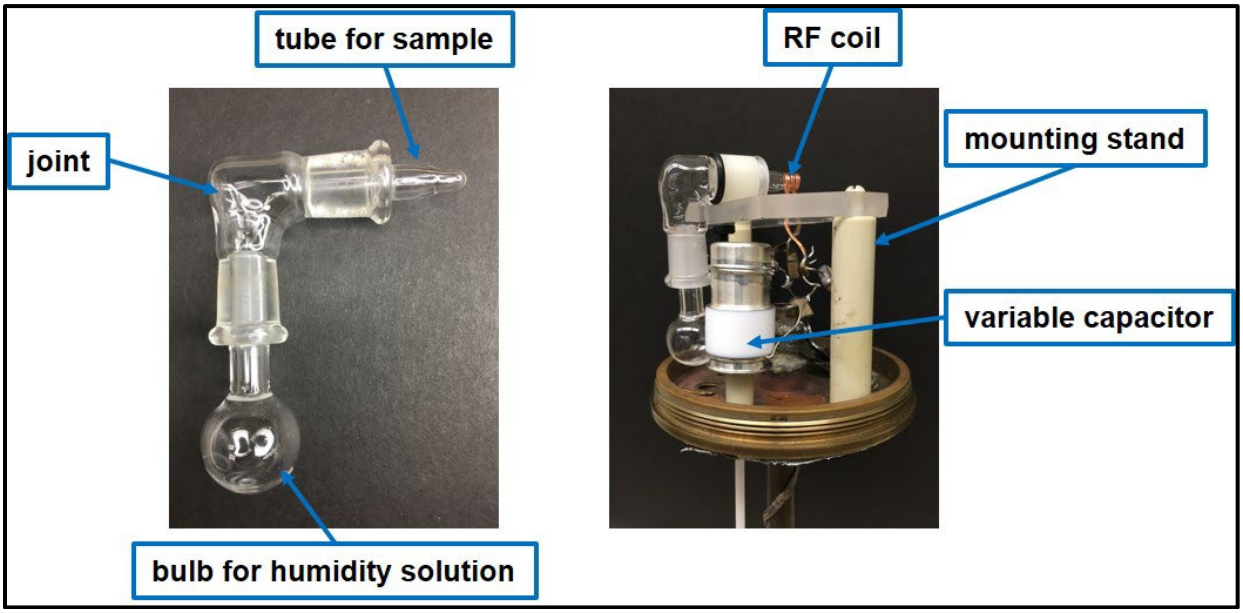

Figure S7. Left: Custom three-piece glassware for constant humidity experiments. Right: incorporation of custom glassware into custom NMR probe head.

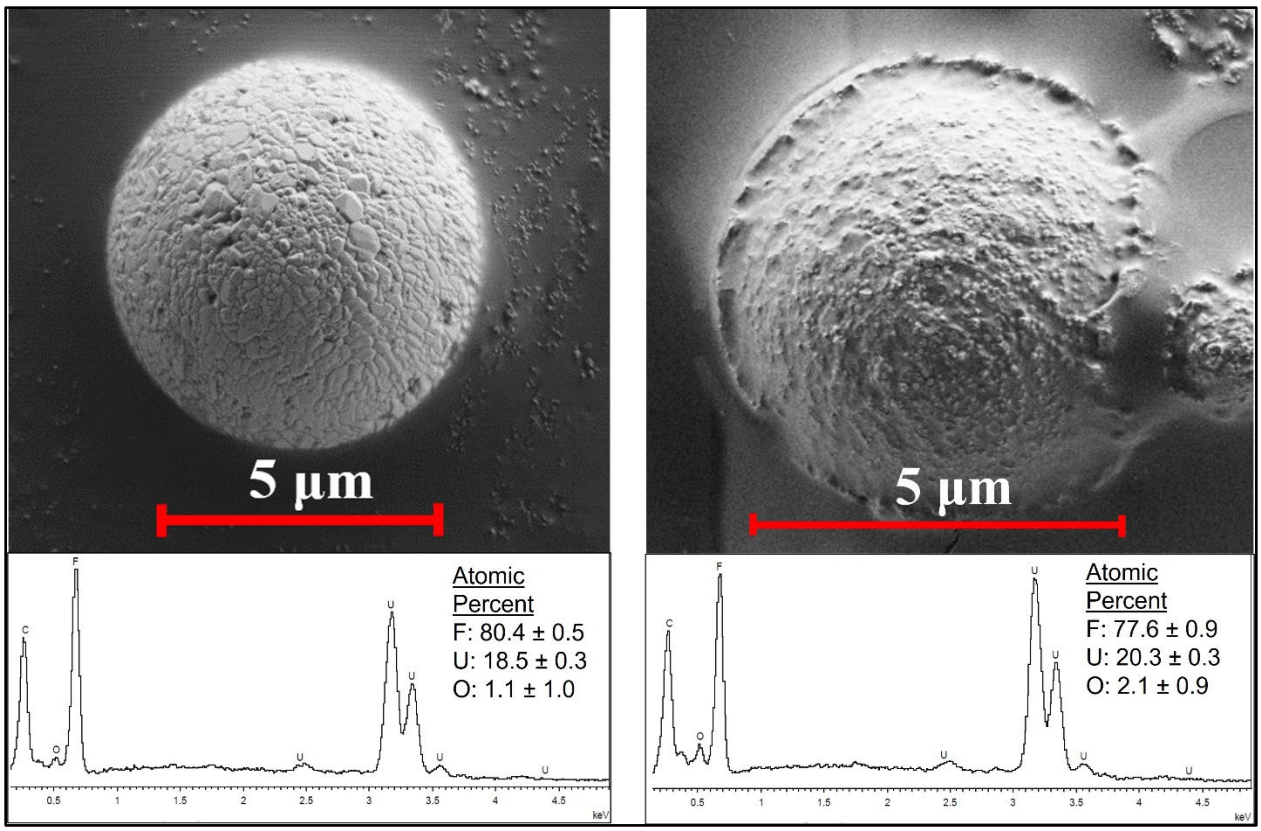

Figure S8. Left: Representative UF_4 sample after exposure to air at 85% RH for 13 days and corresponding EDS spectrum. Right: Representative UF4 sample after exposure to air at 50% RH for 11 days.

Table S1. Previously published Raman resonance bands for UF_4 and several uranium-bearing compounds.

Formula	Laser (nm)	Raman shift bands (cm^{-1})	SI Reference
Anhydrous UF_4	785	59.4, 66.8, 78.9, 91.0, 101.3, 107.2, 115.9, 131.4, 148.5, 170.4, 197.3, 255.8, 296.1, 322.4, 360.8, 603.6	2
$UF_4(H_2O)_{2.5}$	785	82, 95, 106, 118, 156, 185, 235, 257, 282, 320, 333, 340, 364, 427, 3283, 3390, 3481, 3535	3
Hydrated UO_2F_2	514	867, 174	4
Anhydrous UO_2F_2	514	915, 442, 180	4
UO_2	514	445	5
UO_2	514	448, 630, 1104, 1152	6
UO_2	514	445	7
UO_2	514	232, 445, 1151	8
UO_2	488	450, 585, 1595	9
UO_2	488	448, 585, 920, 1150	9
UO_2	785	445, 583, 640, 1160, 1360	9
U_4O_9	---	210, 465	10
U_3O_7	---	210, 465	10
U_3O_7	---	410, 445, 500	7
U_3O_8	514	343, 351, 412, 483, 738, 811	5
U_3O_8	514	236, 342, 408, 480, 752, 798	7
U_3O_8	488	235, 340, 405, 480, 640, 745, 800, 885	9
U_3O_8	514	236, 342, 408, 480, 638, 752, 798, 888	11
γ-UO_3	514	768, 846	5
$UO_2(OH)_2$	---	838, 855	12
Schoepite	1064	843, 845	13

SI References

1. *PDF 4 Database, International Centre for Diffraction Data, Newtown Square, PA, 2015, Card No #01-082-2317*.
2. E. Villa-Aleman and M. S. Wellons, *Journal of Raman Spectroscopy*, 2016, **47**, 865-870.
3. J. H. Christian, C. A. Klug, M. DeVore, E. Villa-Aleman, B. J. Foley, N. Groden, A. T. Baldwin and M. S. Wellons, *Dalton Transactions*, 2021, **50**, 2462-2471.
4. D. P. Armstrong, R. J. Jarabek and W. H. Fletcher, *Applied Spectroscopy*, 1989, **43**, 461-468.
5. M. L. Palacios and S. H. Taylor, *Applied Spectroscopy*, 2000, **54**, 1372-1378.
6. P. R. Graves, *Applied Spectroscopy*, 1990, **44**, 1665-1667.
7. G. C. Allen, I. S. Butler and T. Nguyen Anh, *Journal of Nuclear Materials*, 1987, **144**, 17-19.
8. D. Manara and B. Renker, *Journal of Nuclear Materials*, 2003, **321**, 233-237.
9. S. D. Senanayake, R. Rousseau, D. Colegrave and H. Idriss, *Journal of Nuclear Materials*, 2005, **342**, 179-187.
10. W. Siekhaus, Composition of uranium oxide surface layers analyzed by μ-Raman spectroscopy, *MRS 2003 Fall Meeting, B*oston, MA, USA, 1–5 December, 2005.
11. I. S. Butler, G. C. Allen and N. A. Tuan, *Applied Spectroscopy*, 1988, **42**, 901-902.
12. E. A. Stefaniak, A. Worobiec, S. Potgieter-Vermaak, A. Alsecz, S. Török and R. Van Grieken, *Spectrochimica Acta Part B: Atomic Spectroscopy*, 2006, **61**, 824-830.
13. M. Amme, B. Renker, B. Schmid, M. P. Feth, H. Bertagnolli and W. Döbelin, *Journal of Nuclear Materials*, 2002, **306**, 202-212.